

Excitation functions and isomeric cross section ratios of the $^{63}\text{Cu}(n, \alpha)^{60}\text{Co}^{m,g}$, $^{65}\text{Cu}(n, \alpha)^{62}\text{Co}^{m,g}$, and $^{60}\text{Ni}(n, p)^{60}\text{Co}^{m,g}$ processes from 6 to 15 MeV

F. Cserpák,^{1,2} S. Sudár,^{1,2} J. Csikai,² and S. M. Qaim^{1,*}

¹*Institut für Nuklearchemie, Forschungszentrum Jülich GmbH, D-52425 Jülich, Germany*

²*Institute of Experimental Physics, Kossuth University, 4001 Debrecen, Hungary*

(Received 12 October 1993)

Excitation functions were measured for the $^{63}\text{Cu}(n, \alpha)^{60}\text{Co}^m$, $^{65}\text{Cu}(n, \alpha)^{62}\text{Co}^m$, and $^{65}\text{Cu}(n, \alpha)^{62}\text{Co}^g$ reactions over the neutron energy range of 6.3 to 14.8 MeV. Use was made of the activation technique in combination with high-resolution γ -ray spectroscopy. The neutrons were produced via the $^2\text{H}(d, n)^3\text{He}$ reaction using a deuterium gas target at a variable energy compact cyclotron ($E_n = 6.3$ –11.9 MeV) and via the $^3\text{H}(d, n)^4\text{He}$ reaction using a solid Ti-T target at a neutron generator ($E_n = 13.7$ –14.8 MeV). From the available experimental data isomeric cross section ratios were determined for the isomeric pair $^{60}\text{Co}^{m,g}$ in $^{63}\text{Cu}(n, \alpha)$ and $^{60}\text{Ni}(n, p)$ reactions, and for the pair $^{62}\text{Co}^{m,g}$ in the $^{65}\text{Cu}(n, \alpha)$ reaction. Statistical model calculations taking into account precompound effects were performed for the formation of both the isomeric and ground states of the products. The calculational results on the total (n, p) and (n, α) cross sections agree well with the experimental data; in the case of isomeric states, however, some deviations occur. The experimental isomeric cross section ratios are reproduced only approximately by the calculation; at 15 MeV the spin distribution of the level density has a significant effect on the calculation. For low-lying levels the isomeric cross section ratio depends strongly on the spins of the levels involved and not on their excitation energies. At a given neutron energy the population of the higher spin isomer appears to be higher in the (n, α) process than in the (n, p) reaction.

PACS number(s): 24.60.Dr, 25.40.-h, 28.20.-v

I. INTRODUCTION

Studies of excitation functions of neutron threshold reactions are of considerable importance for testing nuclear models and for practical applications, especially in fusion reactor technology (FRT). Furthermore, isomeric cross section ratios, particularly as a function of energy, are of fundamental interest for studying the spin dependence of the formation of isomeric states. A survey of the available literature (cf. Refs. [1,2]) shows that both the cross section data and the isomeric cross section ratios for many neutron-induced reactions in the energy range of 4–12 MeV are rather scanty. It appeared worthwhile to us to investigate the (n, α) reactions on ^{63}Cu and ^{65}Cu , the available information for which is relatively small. Since copper is an important structural material in FRT, the measured data should furnish useful information on helium-gas production as a function of neutron energy.

Of greater interest, however, are the isomeric cross section ratios. Figure 1 gives simplified schemes of the isomeric levels involved in the product nuclei, namely, ^{60}Co and ^{62}Co (cf. [3]). In both the cases the separation energy between the isomeric levels concerned is small (58.6 and 22 keV, respectively) but the spins differ considerably. In ^{60}Co the ground state has a higher spin than the metastable state but in ^{62}Co it is the other way round. We performed experimental and theoretical studies on the above-mentioned two (n, α) reactions in the neutron energy range 6–15 MeV. Additionally, the $^{60}\text{Ni}(n, p)$ process leading to the formation of the $^{60}\text{Co}^{m,g}$ pair was also investigated.

II. EXPERIMENT

Cross sections were measured by the activation technique, commonly used at both Jülich and Debrecen. This

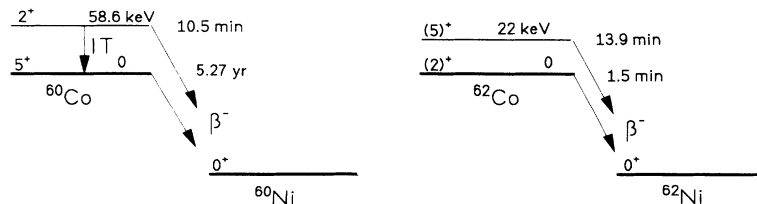


FIG. 1. Simplified level schemes of the isomeric pairs $^{60}\text{Co}^{m,g}$ and $^{62}\text{Co}^{m,g}$.

* Author to whom correspondence should be addressed.

technique is ideally suited for studying the formation of closely spaced nuclear levels, provided their lifetimes are not too short. Some of the salient features relevant to the present measurements are described below.

A. Samples and irradiations

Several types of high-purity natural copper samples were prepared for irradiations. For studies on $^{60}\text{Co}^m$, due to the low energy of the γ ray involved (58.6 keV), thin Cu foils (50 μm , 99.999% pure, Goodfellow, England) of 1.3 or 1.9 cm diam were used. For investigations on $^{62}\text{Co}^m$ and $^{62}\text{Co}^g$, on the other hand, about 5-g Cu metal powder (99.999% pure, Koch-Light, England) was pressed at 10 tonne/cm² and a disk (1.3 cm diam, 0.5 cm thick) was obtained. Monitor foils (Al or Fe, each 200 μm thick) of the same size as the sample were then attached in front and at the back of each sample.

Most of the irradiations were done at the Jülich variable energy compact cyclotron CV28. The quasimonoenergetic neutrons were produced via the $^2\text{H}(d,n)^3\text{He}$ reaction on a D₂ gas target (37 mm long, 1.8×10^5 Pa pressure). The characteristics of this neutron source have been described earlier [4]. The samples were placed in the 0° direction relative to the deuteron beam, at a distance of 1 cm from the back of the beam stop. The energy of the deuteron beam was varied between 4 and 9.5 MeV and the beam current between 2 and 4 μA . For studies on $^{63}\text{Cu}(n,\alpha)^{60}\text{Co}^m$ and $^{65}\text{Cu}(n,\alpha)^{62}\text{Co}^m$ reactions each sample was irradiated together with the monitor foils for 30 min. In studies on $^{65}\text{Cu}(n,\alpha)^{62}\text{Co}^{m,g}$ cross section ratios, however, due to the short half-life of $^{62}\text{Co}^g$ (1.5 min) the irradiation time was limited to 5 min and only relative measurements were done, i.e., no neutron flux monitor was used.

Irradiations with 13.7–14.8-MeV neutrons were done at the neutron generator of the Institute of Experimental Physics, Kossuth University, Debrecen. Monoenergetic neutrons around 14 MeV were produced via the $^3\text{H}(d,n)^4\text{He}$ reaction on a solid Ti-T target. The samples were placed at different angles (0°, 30°, 60°, 90°, 120°) relative to the deuteron beam direction, resulting in different averaged neutron energies within the samples. In each case only the aluminium monitor foil was used. Similar to studies with *dd* neutrons described above, for the $^{63}\text{Cu}(n,\alpha)^{60}\text{Co}^m$ and $^{65}\text{Cu}(n,\alpha)^{62}\text{Co}^m$ reactions cross sections were determined, but for the $^{65}\text{Cu}(n,\alpha)^{62}\text{Co}^{m,g}$ process only ratio measurements were done.

As a check of the $^{63}\text{Cu}(n,\alpha)^{60}\text{Co}^m$ reaction cross section, a single irradiation at $E_n = 9.6$ MeV was done at the variable energy cyclotron MGC-20 of ATOMKI, Debrecen, using a D₂ gas target (50 mm long, 1.5×10^5 Pa pressure). In this case only the aluminium monitor foil was used.

B. Neutron energies and flux densities

In the case of neutrons produced via the $^2\text{H}(d,n)^3\text{He}$ reaction at the D₂ gas target the neutron energies effec-

tive at the monitors as well as the average neutron energies effective at the samples were calculated by a Monte Carlo program (cf. Refs. [5–7]) which takes into account the length of the gas cell, the pressure of the D₂ gas in the cell, and the geometrical parameters of the sample (diameter, length, distance from the beam stop). The double-differential cross sections of the $^2\text{H}(d,n)^3\text{He}$ reaction evaluated by Liskien and Paulsen [8] are the basic parameters for this calculation. The calculated deviations in the energy refer to different emission angles of neutrons.

The neutron flux densities in front and at the back of the sample were determined via monitor reactions $^{27}\text{Al}(n,\alpha)^{24}\text{Na}$ ($T_{1/2} = 15.0$ h, $E_\gamma = 1368.6$ keV, $I_\gamma = 100\%$) and $^{56}\text{Fe}(n,p)^{56}\text{Mn}$ ($T_{1/2} = 2.58$ h, $E_\gamma = 846.8$ keV, $I_\gamma = 98.9\%$). The cross sections were taken from the literature [9].

It is well known that the $^2\text{H}(d,n)^3\text{He}$ reaction at $E_d \geq 5$ MeV is not a really monoenergetic neutron source, the neutron energy spectrum being strongly dependent on the incident deuteron energy and the material of construction of the gas target (cf. Refs. [4,10,11]). The effect of background neutrons becomes significant above 7-MeV incident deuteron energy, especially for reactions of low thresholds. For this reason gas-out measurements were also performed at $E_d = 7.5, 8.5,$ and 9.5 MeV, and two monitor reactions (mentioned above) differing in threshold energies were used.

The deviations between the neutron flux densities calculated from the two monitor reactions, after background (gas-out/gas-in) corrections, ranged between 4 and 20%. The maximum deviations were observed at the highest and the lowest investigated energies. The deviations at the highest energies originated from the high background corrections [at $E_n = 11.94$ MeV, for example, the correction was 47% in the case of the $^{27}\text{Al}(n,\alpha)^{24}\text{Na}$ monitor reaction and 53% for the $^{56}\text{Fe}(n,p)^{56}\text{Mn}$ reaction]. The deviations in the neutron flux densities at the lowest neutron energies were due to uncertainties in monitor cross sections. Since the cross sections of both the monitor reactions change rapidly with the neutron energy, only a few percent deviation between the effective and the estimated energy causes a significant change in the calculated neutron flux density. In the present work we took an average of the neutron flux densities from the two monitor reactions and adopted 3–10% uncertainty in the calculated values.

For neutrons from the $^3\text{H}(d,n)^4\text{He}$ reaction the flux densities were determined via the $^{27}\text{Al}(n,\alpha)^{24}\text{Na}$ reaction. The neutron energies and their deviations were taken from a previous work [12].

C. Measurement of radioactivity

The radioactivity of the irradiated samples and monitor foils was determined via high-resolution γ -ray spectroscopy. The activities of ^{24}Na , ^{56}Mn , and $^{62}\text{Co}^{m,g}$ were measured using HPGe and Ge(Li) detectors. For $^{60}\text{Co}^m$, on the other hand, a thin HPGe detector with a Be window was used. The peak area analysis was done using

the programs MAESTRO I, MAESTRO II, and ACCUSPEC developed for IBM compatible computers.

Due to the short half-lives of the product isotopes, measurements were started within 10 min after irradiations, in cross section ratio measurements within 1 min. In general, for cross section measurements 5 repeated spectra were recorded, and for ratio measurements about 10. The typical measuring times were 5–10 min in the former case, and 2–5 min in the latter.

The decay data adopted for the isomers of ^{62}Co were (cf. Ref. [3]) $^{62}\text{Co}^m$: $T_{1/2}=13.9$ min, $E_\gamma = 1173$ keV, $I_\gamma = 83.8\%$; $^{62}\text{Co}^g$: $T_{1/2} = 1.5$ min, $E_\gamma = 1173$ keV, $I_\gamma = 97.9\%$. Thus, in both the cases the same γ ray was used and the contributions of the two isomers were deduced from an analysis of the decay curve. However, for an additional check, in some cases a few other γ rays were also analyzed.

The measurement of the $^{60}\text{Co}^m$ radioactivity presented more difficulty. This radionuclide decays with a half-life of 10.5 min via isomeric transition IT(99.75%) and β^- emission (0.25%). The 1332-keV γ ray associated with the β^- decay has very low and uncertain intensity. The IT is highly converted. The 58.6-keV γ ray is thus weak ($2.01\pm 0.24\%$) but is measurable. Furthermore, the Co x rays could also be measured. We performed measurements using the 58.6-keV γ ray.

D. Calculation of cross sections and their errors

The cross sections and neutron flux densities were calculated using the well-known activation formula. The count rate was corrected for γ -ray intensity, detector efficiency, geometry, coincidence losses, and self-absorption. In some cases special dead-time correction was needed.

The total efficiency of the detector and the efficiency for the detection of a γ -ray peak were determined as a function of the γ -ray energy and the sample-detector distance using standard point γ sources. For the radial dependence of the efficiency, additional measurements were done and the effective efficiency for the sample was obtained by a numerical integration method described earlier [13].

The major sources of errors in cross section measurements were similar to those described in several earlier publications (cf. [5,7,13]). The error in the excitation function of the monitor reaction was taken as 3–5% and that in the averaging of the neutron flux as 3–10%. The efficiency of the γ detector (incorporating self-absorption, geometry, and pileup) had an uncertainty of 2–6%. The error in the decay data used was < 1% except for the 58.6-keV γ ray of $^{60}\text{Co}^m$ where an uncertainty of 12% was adopted. The major errors involved were due to poor counting statistics (2–25%) and contributions from background neutrons (2–10%). Because of low count rates (10–100 s^{-1}) and short counting time (due to short half-lives) the statistical uncertainty was relatively large in the low neutron energy region. In the high neutron energy range 9–12 MeV the statistical uncertainty was much lower, and the major source of error was the correction due to the background neutrons. We got the nec-

essary information from the gas-out measurements. In the case of the $^{65}\text{Cu}(n, \alpha)^{62}\text{Co}^m$ reaction, for example, the normalized gas-out contribution relative to the gas-in activity amounted to 11.7, 18, and 26% at 10.1-, 11.0-, and 11.94-MeV neutron energy, respectively. The corresponding values for the $^{63}\text{Cu}(n, \alpha)^{60}\text{Co}^m$ reaction were 22, 40, and 68%. Considering the last value, it is evident that a 1% error in the background (for instance, due to the different beam positions during the irradiations) would lead to 2–3% error in the cross section. Nonetheless, such measurements at $E_n = 10$ –12 MeV are worthwhile since the available data are scarce.

Some background neutrons produced via breakup of deuterons on D_2 gas are not taken into account via gas-out measurements. Their contribution is, however, relatively small in the case of threshold reactions investigated in this work. This contribution was calculated from the data of Cabral *et al.* [10]. The total error for each cross section value was obtained by combining the individual errors in quadrature.

E. Calculation of isomeric cross section ratios

The calculation of the isomeric cross section ratio $\sigma_m/(\sigma_m + \sigma_g)$ for the isomeric pair $^{60}\text{Co}^{m,g}$ was straightforward since the σ_m was determined independently by measuring the 58.6-keV γ line of 10.5 min $^{60}\text{Co}^m$, and $\sigma_m + \sigma_g$ after the complete decay of $^{60}\text{Co}^m$ to 5.27 yr $^{60}\text{Co}^g$. Regarding the isomeric pair $^{62}\text{Co}^{m,g}$, however, some difficulty was encountered since the two isomeric states decay independently to the product nucleus ^{62}Ni . We chose to investigate the 1173-keV γ line (see above) which is emitted in the decay of both the isomers but with different abundances. After an irradiation, repeated measurements were done and the γ -ray spectra were recorded. Then, peak areas of the 1173-keV γ line were obtained as a function of cooling and measuring times.

From general principles, the peak area (A_{peak}^i) is given by the expression

$$A_{\text{peak}}^i = I_{\gamma m} f_{cm} \varepsilon_p N_m(0) e^{-\lambda_m t_c^i} (1 - e^{-\lambda_m t^i}) + I_{\gamma g} f_{cg} \varepsilon_p N_g(0) e^{-\lambda_g t_c^i} (1 - e^{-\lambda_g t^i}), \quad (1)$$

where m and g refer to the metastable and the ground state, I_γ is the γ -ray abundance, ε_p is the peak efficiency, f_c is the coincidence summing correction factor, $N(0)$ is the number of radioactive atoms at the end of irradiation, λ is the decay constant, t_c^i is the cooling time interval measured from the end of irradiation to the beginning of measurement, and t^i is the measuring time interval.

The A_{peak}^i values ($i = 1, 2, \dots, n$) obtained experimentally were fitted by a curve using the least-squares method, with the weighting factor $W^i = A_{\text{peak}}^i / \Delta A_{\text{peak}}^i$. In general, this fitting worked out very well up to $E_n = 10$ MeV and the values for $N_m(0)$ and $N_g(0)$ were obtained within an estimated error of 2%. The cross section ratio was then calculated using the expression

$$\frac{\sigma_m}{\sigma_g} = \frac{N_m(0)}{N_g(0)} \frac{\lambda_m}{\lambda_g} \frac{(1 - e^{-\lambda_g t_{ir}})}{(1 - e^{-\lambda_m t_{ir}})}, \quad (2)$$

where t_{ir} denotes the time of irradiation.

At neutron energies above 10 MeV, due to the opening of several other strong reaction channels, a further correction may become mandatory. Around 14 MeV, for example, the $^{63}\text{Cu}(n, 2n)^{62}\text{Cu}$ reaction dominates ($\sigma = 1$ b). Since the (n, α) cross section is low and since a rapid radiochemical separation of radiocobalt from copper matrix activity could not be applied, it was necessary to measure the irradiated sample close to the detector. The high activity of ^{62}Cu ($T_{1/2} = 9.8$ min) caused a significant dead time which decreased with time. A correction for the changing dead time was therefore developed in the form

$$D(t) = D(0)e^{-\lambda^*t}, \quad (3)$$

where $D(t)$ is a correction factor at time t , $D(0)$ is the value of the factor at the end of irradiation, and λ^* is the constant of the decay which causes the dead time.

Using a pulse generator of constant frequency connected to the preamplifier we could determine the averaged dead times of the measurements. During the course of repeated spectrum measurements after an irradiation (mentioned above), dead times were also registered. Fitting a curve to those measured dead-time values we got $D(0)$ and λ^* values. In general, for measured dead times of 20%, the fitted values agreed within 5%. For higher dead times of up to 30%, the agreement was within 30%. The dead-time function thus developed was used to calculate the cross section ratio at 14.12 MeV and higher neutron energies.

III. NUCLEAR MODEL CALCULATIONS

Cross section calculations were done using the statistical model taking into account the preequilibrium effects via the exciton model as described in the code STAPRE [14]. The contribution of the direct reactions can be estimated to be less than 10%; therefore, they were not considered. Neutron, proton, alpha, and deuteron emission was taken into account and the transmission coefficients for these particles were calculated by the optical-model code SCAT-2 [15]. The parameters for the optical model (OM) were chosen from a global parameter set. For the neutron the OM parameter set of Becchetti and Greenlees [16], while for the proton and deuteron the OM parameter set of Perey [17] were used. In the case of alpha particles the OM parameters of McFadden and Satchler [18] modified by Uhl *et al.* [19] were used. For the energy and mass dependence of the effective matrix element, $|M|^2 = (FM)A^{-3}E^{-1}$ formula was used with value of $FM = 300$. The separation energies of the emitted particles were taken from Ref. [20].

The energies, spins, parities, and branching ratios of the discrete levels were selected from Nuclear Data Sheets [21]. In some cases, especially for ^{62}Co , the branching ratio data were very scanty; therefore branching ratios for the known levels were calculated using the transmission coefficients of the photons. In the continuum region the level density was calculated by the backshifted formula [22] and the level-density parameters given in Ref. [22]

were used. In cases where these parameters were not available, they were estimated from the systematics and from the values of the neighboring isotopes. Occasionally the level density parameters \mathbf{a} and Δ were varied within their uncertainties to improve the reproduction of the cross sections. The spin distribution of the level density was characterized by the ratio of the effective moment of inertia Θ_{eff} to rigid-body moment of inertia Θ_{rig} ($\eta = \Theta_{\text{eff}}/\Theta_{\text{rig}}$). The calculations were performed for $\eta = 1.0$ and 0.5. The transmission coefficients of photons were calculated from the γ -ray strength functions. For $E1$ radiation the Brink-Axel model with global parameters, and for the $M1$, $E2$, $M2$, $E3$, and $M3$ radiations the Weisskopf model was used.

IV. RESULTS AND DISCUSSION

A. Cross sections and excitation functions

The measured activation cross sections together with their total uncertainties are given in Table I. Although natural copper was used as target material, the contribution of the $^{63}\text{Cu}(n, 2p)^{62}\text{Co}^{m,g}$ process to the $^{65}\text{Cu}(n, \alpha)^{62}\text{Co}^{m,g}$ process should be $< 1\%$, since at 14 MeV the estimated $(n, 2p)$ cross section amounts to $< 25 \mu\text{b}$ as compared to 5 mb for the (n, α) process. As mentioned above, the data for the $^{63}\text{Cu}(n, \alpha)^{60}\text{Co}^m$ and $^{65}\text{Cu}(n, \alpha)^{62}\text{Co}^m$ processes were measured directly; for the $^{65}\text{Cu}(n, \alpha)^{62}\text{Co}^g$ reaction, however, they were deduced from the $^{62}\text{Co}^m/^{62}\text{Co}^g$ ratio measurements. Except for a single value for the $^{63}\text{Cu}(n, \alpha)^{60}\text{Co}^m$ reaction at 8.2 MeV [23], all the data reported here over the neutron energy range 6–12 MeV have been measured for the first time.

The excitation functions of the $^{63}\text{Cu}(n, \alpha)^{60}\text{Co}^m$, $^{63}\text{Cu}(n, \alpha)^{60}\text{Co}^{m+g}$, $^{65}\text{Cu}(n, \alpha)^{62}\text{Co}^m$, and $^{65}\text{Cu}(n, \alpha)^{62}\text{Co}^g$ reactions are given in Figs. 2–5, respectively. For the $^{63}\text{Cu}(n, \alpha)^{60}\text{Co}^m$, $^{65}\text{Cu}(n, \alpha)^{62}\text{Co}^m$, and $^{65}\text{Cu}(n, \alpha)^{62}\text{Co}^g$ reactions, in addition to our own experimental data, the available literature data, mainly around 14 MeV (cf. [23–27]), are also shown. For the $^{63}\text{Cu}(n, \alpha)^{60}\text{Co}^{m+g}$ process, on the other hand, good measurements existed in the literature over the whole neutron energy range up to 15 MeV (cf. [2, 28, 29]) and Fig. 3 is based on those data. The results of nuclear model calculations performed in the present study are also reproduced in Figs. 2–5 for comparison.

For the $^{63}\text{Cu}(n, \alpha)^{60}\text{Co}^m$ reaction (Fig. 2) the experimental and theoretical data agree well up to 12 MeV. Around 14 MeV, however, the calculated cross sections are appreciably higher than the experimental values, though the calculation with $\eta = 1.0$ gives values closer to the experimental data. On the other hand, the experimental results both from our measurements and from [27] show considerable fluctuations, so the deviation between experiment and theory may simply be due to large errors in the experimental data for this reaction.

The experimental and theoretical results for the $^{63}\text{Cu}(n, \alpha)^{60}\text{Co}^{m+g}$ process (Fig. 3) agree very well over the whole energy range. Calculations with $\eta = 1.0$ gave better results for this nuclear reaction as well.

TABLE I. Measured and deduced fast neutron-induced activation cross sections.

$\langle E_n \rangle^a$ (MeV)	$^{63}\text{Cu}(n, \alpha)^{60}\text{Co}^m$	$^{65}\text{Cu}(n, \alpha)^{62}\text{Co}^m$	$^{65}\text{Cu}(n, \alpha)^{62}\text{Co}^{m,g}$ $R \left[\frac{\sigma(m)}{\sigma(g)} \right]$	$^{65}\text{Cu}(n, \alpha)^{62}\text{Co}^g$
	σ (mb)	σ (mb)		σ (mb)
6.32±0.14	4.4±0.7	0.02±0.006	0.37±0.15	0.056±0.03
6.82±0.14	6.1±0.6			
7.31±0.14	10.6±1.5	0.13±0.014	0.42±0.13	0.31±0.09
7.79±0.15	10.5±0.6	0.27±0.08		
8.26±0.15	13.6±1.6	0.38±0.07	0.47±0.07	0.81±0.2
9.18±0.16	17.5±2.6	0.86±0.09	0.48±0.06	1.82±0.3
9.60±0.17	14.9±2.2			
10.10±0.17	20.1±1.2	1.26±0.25	0.54±0.04	2.34±0.5
11.00±0.18	21.7±4.3	1.85±0.25	0.56±0.03	3.35±0.3
11.94±0.18	17.2±2.7	3.47±0.45	0.73±0.07	4.75±0.7
13.75±0.20	8.3±1.6		0.76±0.04	
14.12±0.16	14.6±3.6	4.56±0.63	0.95±0.05	5.88±0.9
14.45±0.15	8.2±3.0	6.44±0.63	1.18±0.14	5.43±0.9
14.71±0.30	16.36±2.6	5.31±0.56	1.15±0.06	4.26±0.5
14.80±0.34		7.57±1.06		

^aThe deviations do not describe errors in the energy scale; they show energy spreads due to angle of emission.

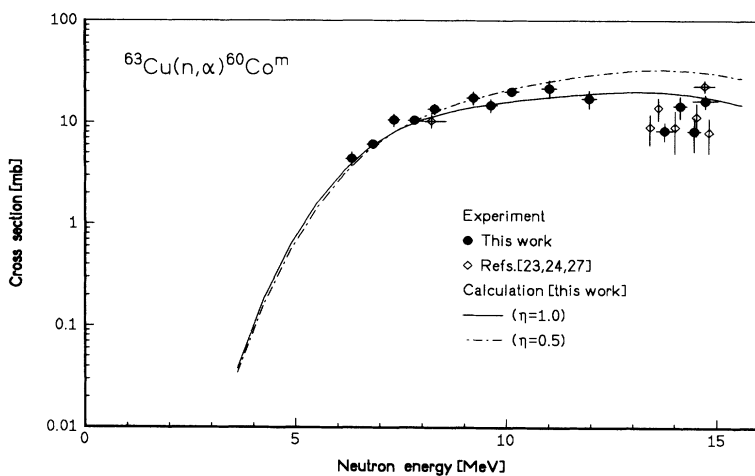


FIG. 2. Excitation function of the $^{63}\text{Cu}(n, \alpha)^{60}\text{Co}^m$ ($T_{1/2} = 10.5$ min) reaction.

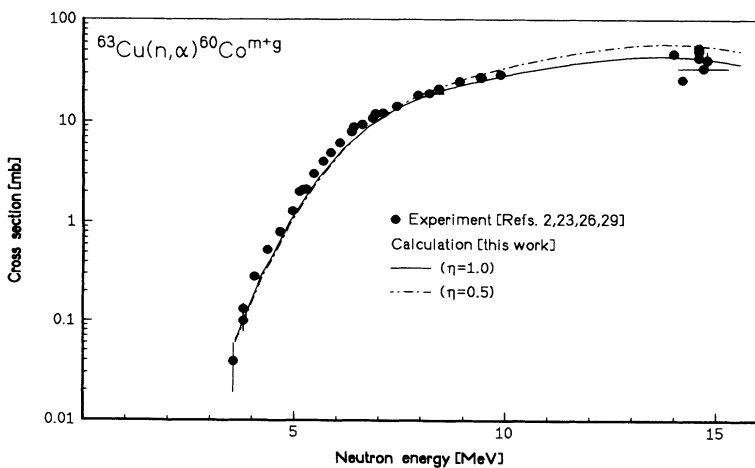


FIG. 3. Excitation function of the $^{63}\text{Cu}(n, \alpha)^{60}\text{Co}^{m+g}$ ($T_{1/2} = 5.27$ yr) process.

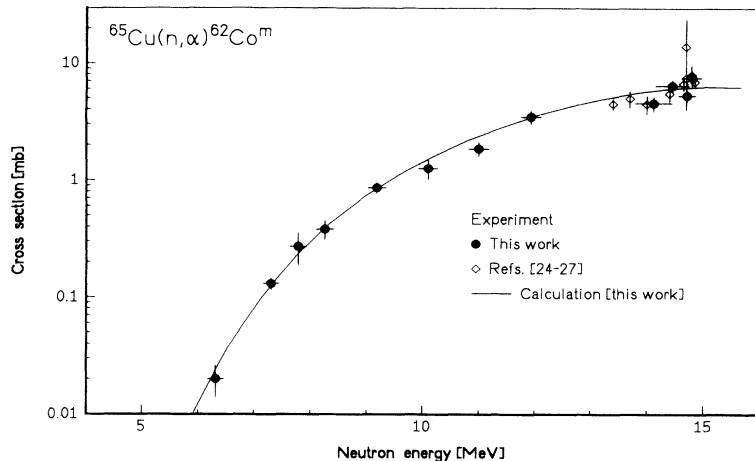


FIG. 4. Excitation function of the $^{65}\text{Cu}(n, \alpha)^{62}\text{Co}^m$ ($T_{1/2} = 13.9$ min) reaction.

We therefore adopted this value in other calculations. The experimental and theoretical data for the reactions $^{65}\text{Cu}(n, \alpha)^{62}\text{Co}^m$ (Fig. 4) and $^{65}\text{Cu}(n, \alpha)^{62}\text{Co}^g$ (Fig. 5) are also in agreement over the whole investigated energy range. It is therefore concluded that the nuclear model calculations described here reproduce the experimental excitation functions of the (n, α) reactions on copper reasonably well. This applies particularly to the total (n, α) cross section, i.e., the sum of σ_m and σ_g .

We consider now in detail the (n, p) reaction on ^{60}Ni which also leads to the isomeric pair $^{60}\text{Co}^{m,g}$ (studied in the present work). The excitation functions of the reactions $^{60}\text{Ni}(n, p)^{60}\text{Co}^m$ and $^{60}\text{Ni}(n, p)^{60}\text{Co}^{m+g}$ were measured recently up to 10 and 12 MeV, respectively, under a Jülich-Debrecen cooperative effort [30]. Over this energy range almost no data existed for the $^{60}\text{Ni}(n, p)^{60}\text{Co}^m$ reaction, and those available for the $^{60}\text{Ni}(n, p)^{60}\text{Co}^{m+g}$ process were very discrepant. A similar study performed on the latter reaction under a Los Alamos-Vienna cooperation [31,32] agreed with our results. The excitation functions of the $^{60}\text{Ni}(n, p)^{60}\text{Co}^m$ and $^{60}\text{Ni}(n, p)^{60}\text{Co}^{m+g}$ reactions, based on the most recent data up to 12.5 MeV [30–32], and incorporating all the other data available at energies around 14 MeV (cf. [2]), are shown in Figs. 6 and 7, respectively. For both the processes there is a

large scatter in the data at neutron energies around 14 MeV. The results of nuclear model calculations done in the present work are also reproduced. Evidently, the total (n, p) cross section (i.e., $\sigma_m + \sigma_g$), is described well by the theory (cf. Fig. 7); the cross section for the formation of the isomeric state ($^{60}\text{Co}^m$) is, however, somewhat underestimated by the theory (cf. Fig. 6).

B. Helium-production cross sections

A comparison of the magnitudes of the four helium-producing reactions on $^{\text{nat}}\text{Cu}$ up to 11 MeV, namely, $^{63}\text{Cu}(n, \alpha)^{60}\text{Co}^m$, $^{63}\text{Cu}(n, \alpha)^{60}\text{Co}^{m+g}$, $^{65}\text{Cu}(n, \alpha)^{62}\text{Co}^m$, and $^{65}\text{Cu}(n, \alpha)^{62}\text{Co}^g$, shows that by far the largest contribution is furnished by the $^{63}\text{Cu}(n, \alpha)^{60}\text{Co}^{m+g}$ reaction which includes the amount formed via the $^{63}\text{Cu}(n, \alpha)^{60}\text{Co}^m \xrightarrow{\text{IT}} ^{60}\text{Co}^g$ process. The contributions of the other two reactions are relatively small. By normalizing cross sections to the respective abundances of ^{63}Cu and ^{65}Cu in natural copper, it was possible to obtain averaged helium emission cross sections for natural copper. The values thus deduced for $E_n \leq 11$ MeV were compared with the cross section data obtained via helium emission spectral measurements

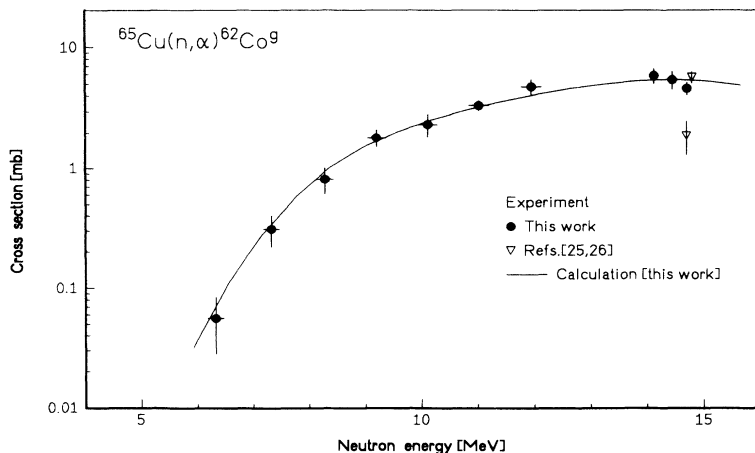


FIG. 5. Excitation function of the $^{65}\text{Cu}(n, \alpha)^{62}\text{Co}^g$ ($T_{1/2} = 1.5$ min) reaction.

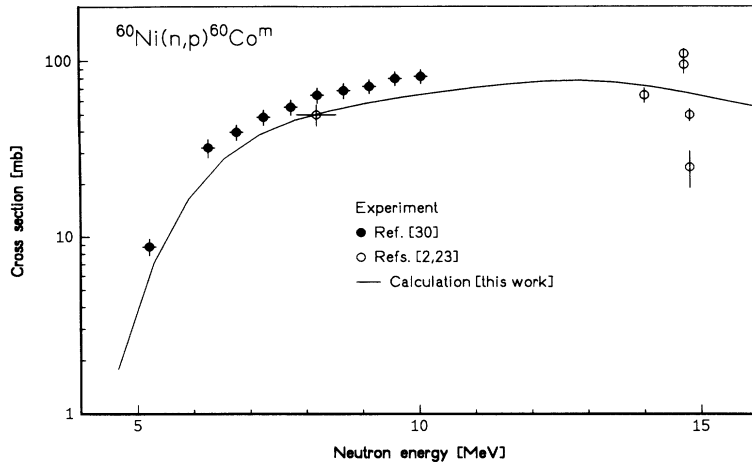


FIG. 6. Excitation function of the $^{60}\text{Ni}(n,p)^{60}\text{Co}^m$ ($T_{1/2} = 10.5$ min) reaction.

[33,34]. In general, the data obtained via the two techniques agreed within 25%. At neutron energies above 11 MeV the activation technique is less reliable for estimating total helium emission from copper since other competing reactions like $(n,n'\alpha)$ also set in (cf. [35]). At 14 MeV the spectral and mass spectrometric techniques have been successfully applied for this purpose (cf. [36,37]).

C. Isomeric cross section ratios

The experimental results on the isomeric cross section ratios $\sigma_m/(\sigma_m + \sigma_g)$ for the isomeric pair $^{60}\text{Co}^{m,g}$ produced in the $^{60}\text{Ni}(n,p)$ and $^{63}\text{Cu}(n,\alpha)$ reactions are given in Figs. 8 and 9, respectively. The cross sections for the formation of the ground state were taken from Refs. [2,28–32], and those for the metastable state from our own measurements [30, this work] and the literature [2,23,24,27]. Around 14 MeV, results of only those literature studies are shown where cross sections of both the metastable and the ground state were measured. The results of nuclear model calculations done in the present work are also shown. The experimental isomeric cross section ratio is high up to 10 MeV, in both the (n,p) and (n,α) processes; it shows some decrease at the high-

est investigated energies of about 14 MeV. This implies that at relatively low projectile energies the low spin isomer (2^+) is preferentially populated; at higher energies, however, the contribution of the high spin isomer (5^+) increases. This result is in conformity with the previous observations on several isomeric states (cf. [38–42]). Furthermore, a comparison of the ratios in the (n,p) and (n,α) reactions suggests that the α emission leads to slightly enhanced population of the higher spin isomer than the p emission. The nuclear model calculations give somewhat lower isomeric cross section ratios in both the (n,p) and (n,α) processes. At energies around 15 MeV the calculated ratios are dependent on the value of η used (cf. also Refs. [39,42]).

The isomeric cross section ratios for the isomeric pair $^{62}\text{Co}^{m,g}$ are given in Fig. 10. Since the two isomers decay independently, we show the data as both σ_m/σ_g and $\sigma_m/(\sigma_m + \sigma_g)$. The ratio is low at low projectile energies but increases significantly with the increasing incident energy. Evidently, here also the low spin isomer (2^+) is preferentially populated, although in this case (contrary to $^{60}\text{Co}^{m,g}$) it is the ground state of the product nucleus. The nuclear model calculation reproduces the shape and the magnitude of the isomeric cross section ratio fairly well.

From the experimental and theoretical studies reported

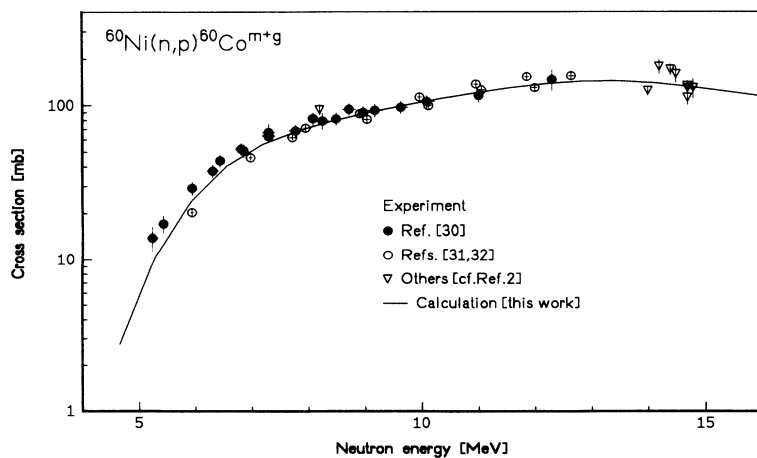


FIG. 7. Excitation function of the $^{60}\text{Ni}(n,p)^{60}\text{Co}^{m+g}$ ($T_{1/2} = 5.27$ yr) process.

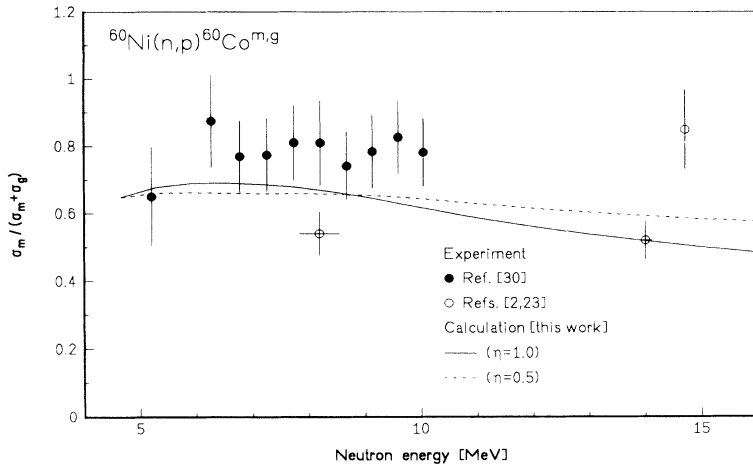


FIG. 8. Isomeric cross section ratio for the isomeric pair $^{60}\text{Co}^{m,g}$, formed via (n,p) reaction on ^{60}Ni , plotted as a function of incident neutron energy. The metastable state has a spin of 2^+ and the ground state 5^+ .

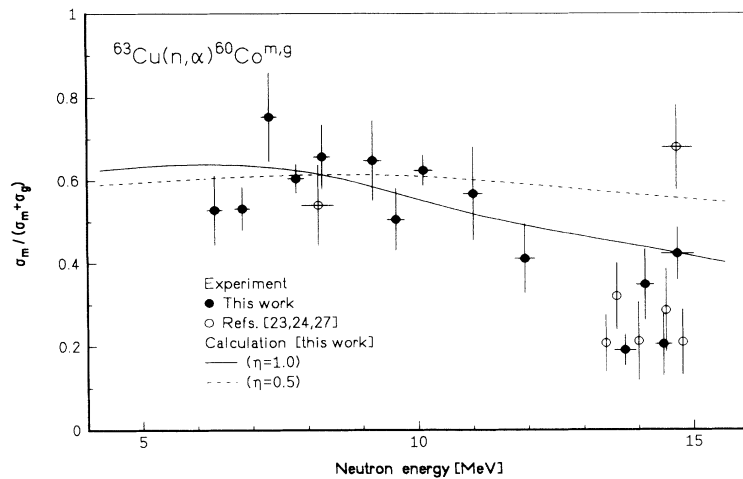


FIG. 9. Isomeric cross section ratio for the isomeric pair $^{60}\text{Co}^{m,g}$, formed via (n,α) reaction on ^{63}Cu , plotted as a function of incident neutron energy.

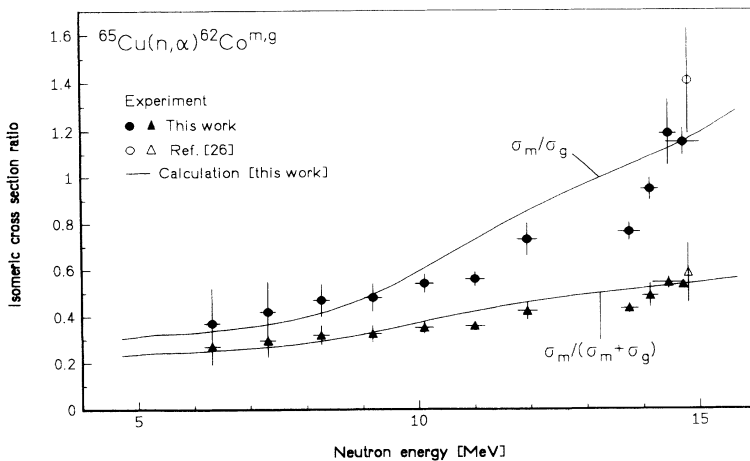


FIG. 10. Isomeric cross section ratio for the isomeric pair $^{62}\text{Co}^{m,g}$ formed via (n,α) reaction on ^{65}Cu , plotted as a function of incident neutron energy. The metastable state has a spin of 5^+ and the ground state 2^+ .

in this work it is concluded that at a given incident neutron energy the isomer distribution in the product nucleus is primarily governed by the spins of the isomeric levels involved and not by their excitation energies. Even for closely spaced levels the isomeric cross section ratio may differ considerably if their spins are different. At a given incident neutron energy the high spin isomer appears to be preferentially populated in the (n, α) process than in the (n, p) reaction. The nuclear model calculation of the isomeric cross section ratio is influenced by the spin distribution of the level density, characterized by the effective moment of inertia.

ACKNOWLEDGMENTS

We thank Professor G. Stöcklin for his active support of this collaborative research program between Jülich and Debrecen. Acknowledgment is made to the crews of the compact cyclotron (Jülich) and neutron generator (Debrecen) for numerous irradiations, and S. Spellerberg, S. Dobránszky, and Gy. Ambrus for experimental assistance. This work was partly supported by the German-Hungarian bilateral agreement [No. 13 ($\times 237.1$)], Hungarian Research Foundation (Contract No. 1734/91), and the Széchenyi István Foundation.

- [1] *CINDA-A (1935-1987), The Index to Literature and Computer Files on Microscopic Neutron Data* (IAEA, Vienna, 1990).
- [2] V. McLane, C. L. Dunford, and P. F. Rose, *Neutron Cross Sections* (Academic, New York, 1988), Vol. 2.
- [3] E. Browne and R. B. Firestone, in *Table of Radioactive Isotopes*, edited by V. S. Shirley (Wiley, New York, 1986).
- [4] S. M. Qaim, R. Wölflé, M. M. Rahman, and H. Ollig, *Nucl. Sci. Eng.* **88**, 143 (1984).
- [5] S. M. Qaim and R. Wölflé, *Nucl. Sci. Eng.* **96**, 52 (1987).
- [6] I. Birn, "NEUT" - Ein Programm zur Berechnung von Neutronenspektren erzeugt durch die $D(d, n)^3\text{He}$ -Reaktion in einem Gastarget am Zyklotron, KFA Jülich, Internal Report INC-IB-1, 1992.
- [7] I. Birn and S. M. Qaim, *Nucl. Sci. Eng.*, in press.
- [8] H. Liskien and A. Paulsen, *Nucl. Data Tables* **11**, 569 (1973).
- [9] IRDF (International Radiation Dosimetry File) (1990), issued by the International Atomic Energy Agency, Vienna, as a computer file.
- [10] S. Cabral, G. Börker, H. Klein, and W. Mannhart, *Nucl. Sci. Eng.* **106**, 308 (1990).
- [11] Á. Grallert, J. Csikai, S. M. Qaim, and J. Knieper, *Nucl. Instrum. Methods A* **334**, 154 (1993).
- [12] P. Raics, Doctoral dissertation, Kossuth Lajos University, 1979.
- [13] S. M. Qaim, F. Cserpák, and J. Csikai, *Appl. Radiat. Isotopes* **43**, 1065 (1992).
- [14] M. Uhl and B. Strohmaier, Computer code for particle-induced activation cross section and related quantities, Institut für Radiumforschung und Kernphysik Report 76/01, 1976, and Addenda to this report. See also B. Strohmaier and M. Uhl, International Atomic Energy Agency Report IAEA-SMR-43, 1980, p. 313.
- [15] O. Bersillon, Centre d'Etudes de Bruyères-le-Châtel, Report CEA-N-2227, 1981.
- [16] F. D. Becchetti and G. W. Greenlees, *Phys. Rev.* **182**, 1190 (1969).
- [17] F. G. Perey, *Phys. Rev.* **131**, 745 (1962).
- [18] L. McFadden and G. R. Satchler, *Nucl. Phys.* **84**, 177 (1966).
- [19] M. Uhl, H. Gruppelaar, H. A. J. van der Kamp, J. Kopecky, and D. Nierop, in *Proceedings of the International Conference on Nuclear Data for Science and Technology*, Jülich, 1991, edited by S. M. Qaim (Springer-Verlag, Berlin, 1992), p. 924.
- [20] A. H. Wapstra and K. Bos, *Atomic Data Nucl. Data Tables* **19**, 215 (1977).
- [21] R. L. Auble, *Nucl. Data Sheets* **28**, 559 (1979); P. Andersson, L. P. Ekström, and J. Lyttlans, *ibid.* **48**, 251 (1986); **39**, 641 (1983); M. L. Halbert, *ibid.* **26**, 5 (1979).
- [22] W. Dilg, W. Schantl, H. Vonach, and M. Uhl, *Nucl. Phys.* **A217**, 269 (1973).
- [23] A. Paulsen, *Z. Phys.* **205**, 226 (1967).
- [24] I. Kantele and D. G. Gardner, *Nucl. Phys.* **35**, 353 (1962).
- [25] E. T. Bramlitt and R. W. Fink, *Phys. Rev.* **131**, 2649 (1963).
- [26] O. I. Artem'ev, I. V. Kazachevskii, V. N. Levkovskii, V. L. Poznyak, and V. F. Rentov, *At. Energ.* **49**, 195 (1980).
- [27] T. Katoh, K. Kawade, and H. Yamamoto, Japan Atomic Energy Research Institute Report JAERI-M, 89-083, 1989.
- [28] Evaluated Nuclear Data File (ENDF)/B-V, Dosimetry file (1979), issued by National Nuclear Data Center, Brookhaven National Laboratory, received as computer listing in Nuclear Energy Agency Data Bank, Saclay, France.
- [29] G. Winkler, D. L. Smith, and J. W. Meadows, *Nucl. Sci. Eng.* **76**, 30 (1980).
- [30] S. Sudár, J. Csikai, S. M. Qaim, and G. Stöcklin, in *Proceedings of the International Nuclear Conference on Nuclear Data for Science and Technology* [19], p. 291.
- [31] H. Vonach, M. Wagner, and R. C. Haight, in *Proceedings of the Specialists' Meeting on Neutron Activation Cross Sections for Fission and Fusion Energy Applications*, Argonne, 1989, edited by M. Wagner and H. Vonach (OECD, Paris, 1990), p. 165.
- [32] M. Wagner, H. Vonach, and R. C. Haight, in *Proceedings of the International Conference on Nuclear Data for Science and Technology* [19], p. 358.
- [33] M. Ahmad, C. E. Brient, P. M. Egun, S. M. Grimes, S. Saraf, and H. Satyanarayana, *Nucl. Sci. Eng.* **95**, 296 (1987).
- [34] E. Wattecamps, in *Proceedings of the International Conference on Nuclear Data for Science and Technology* [19], p. 310.
- [35] S. M. Qaim, *Nucl. Phys.* **A458**, 237 (1986).
- [36] S. M. Grimes, R. C. Haight, K. R. Alvar, H. H. Barschall, and R. R. Borchers, *Phys. Rev. C* **19**, 2127 (1979).
- [37] D. W. Kneff, H. Farrar IV, F. M. Mann, and R. E. Schenter, *Nucl. Technol.* **49**, 498 (1980).
- [38] A. Mannan and S. M. Qaim, *Phys. Rev. C* **38**, 630 (1988).
- [39] S. M. Qaim, A. Mushtaq, and M. Uhl, *Phys. Rev. C* **38**, 645 (1988).
- [40] S. M. Qaim, M. Ibn Majah, R. Wölflé, and B. Strohmaier, *Phys. Rev. C* **42**, 363 (1990).
- [41] N. I. Molla, S. M. Qaim, and M. Uhl, *Phys. Rev. C* **42**, 1540 (1990).
- [42] S. Sudár, F. Szelecsényi, and S. M. Qaim, *Phys. Rev. C* **48**, 3115 (1993).